Aerospace Science and Technology 58 (2016) 197–206

Contents lists available at ScienceDirect

Aerospace Science and Technology

www.elsevier.com/locate/aescte

Stress concentration at the corners of polygonal hole in finite plate

Mihir M. Chauhan [a], Dharmendra S. Sharma [b,*]

[a] Institute of Technology, Nirma University, Ahmedabad 382481, Gujarat, India
[b] Faculty of Technology and Engineering, The Maharaja Sayajirao University of Baroda, Vadodara 390001, Gujarat, India

ARTICLE INFO

Article history:
Received 20 May 2016
Received in revised form 3 August 2016
Accepted 13 August 2016
Available online 20 August 2016

Keywords:
Anisotropic material
Boundary collocation
Complex variable
Finite plate
Polygonal hole
Stress concentration factor

ABSTRACT

A generalized formulation to determine the stresses around the polygonal shaped hole in anisotropic finite plate is presented in the paper. The stress concentration at the rounded corners of the polygonal hole in finite plate subjected to in-plane loading is derived using complex variable approach in conjunction with boundary collocation method. The influence of plate size, hole geometry and location, material anisotropy and loading conditions on the stress concentration around the polygonal hole is studied and presented in the paper. The results obtained through present method are validated by comparing with literature and finite element solutions.

1. Introduction

The polygonal shaped cutouts are provided in a plate like structural components for the requirement of service in many engineering applications like windows panels of aircraft, openings in marine vehicles, opening for fixtures in space vehicle, perforated plates, etc. which are generally made of laminated composite materials. The presence of the sharp corners of polygonal hole adversely affects the stress field in the plate when subjected to various loading. The material anisotropy and the size of plate also affect the stresses in the plate and raise the stress concentration around the hole. The high stress concentration may lead to the catastrophic failure of the components. To understand the catastrophe of the component it is necessary to estimate the stresses produced in the plate under different loading conditions.

Various methods have been used by different researchers to determine the stresses around the cutout in a plate. Chen [1] used special finite element method to obtain the stress concentration around hole in infinite plate. Wang et al. [2] used complex boundary integral method to obtain the stress field in an infinite plate with multiple circular hole. Muskhelishvili [3] has introduced a complex variable method to solve the problems of theory of elasticity. Savin [4], Lekhnitskii [5], Rao et al. [6], Sharma [7–9], Batista [10], Rezaeepazhand and Jafari [11–13], Daoust and Hoa [14], etc. have presented the analytical solution to estimate the stress concentration around various shapes of polygonal hole for isotropic and anisotropic plate subjected to remote loading using Muskhelishvili's [3] complex variable approach. The size of the plate is considered infinite compared to the size of hole in all these literatures. But in many practical cases the size of plate is finite for which these solutions are inappropriate.

The derivation of the stress field in finite plate with circular and elliptical hole is presented by Ogonowski [15], Madenci et al. [16], Xu et al. [17], Lin and Ko [18], Durelli et al. [19], etc. for anisotropic and isotropic materials. The solution of deriving the stresses around rectangular hole and regular polygonal hole in finite plate is presented by Pan et al. [20] and Jafari and Ardalani [21] respectively for isotropic material. For anisotropic finite plate, the solutions of stress concentration factor around rectangular hole and stress intensity factors at cusp of hypocycloidal hole are presented by Chauhan and Sharma [22,23]. All these solutions have utilized the boundary collocation method proposed by Bowie and Neal [24] and Newman [25]. The study of the existing literatures reveals that the solution of deriving stresses around regular polygonal hole in anisotropic finite plate has still not been attempted, within the best of author's knowledge.

An attempt is made here to derive a generalized formulation to obtain the stresses around the regular polygonal shaped hole in anisotropic finite plate under the action of in-plane loading. The stress functions are derived using complex variable approach in conjunction with boundary collocation method. The effect of plate size, hole geometry, hole orientation and location, material properties and loading conditions on the stresses around the hole is also studied.

* Corresponding author.
E-mail address: dss_iitb@yahho.com (D.S. Sharma).

http://dx.doi.org/10.1016/j.ast.2016.08.014
1270-9638/

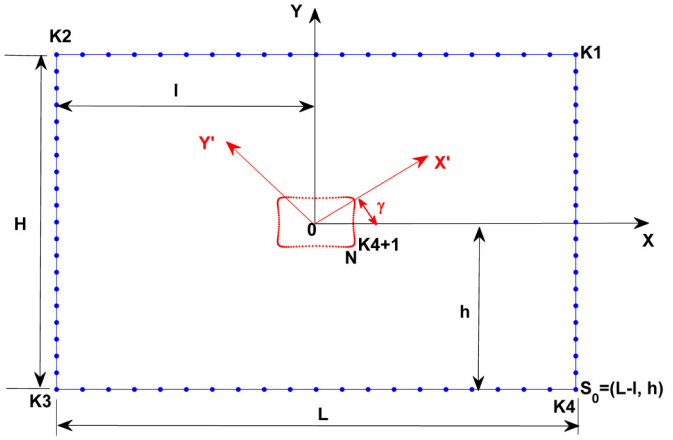

Fig. 1. Collocation points on the plate and hole boundary.

2. Analytical formulation

A thin rectangular anisotropic plate of length L and height H with a polygonal hole located at l and h distance from the bottom and left edge of the plate respectively is under the application of in-plane loading along X′0Y′ frame, as shown in Fig. 1. Assuming the plane stress condition, the stress components in an anisotropic plate [5] can be obtained as,

$$\begin{aligned}\sigma_x &= 2\,\mathrm{Re}\left[\sum_{j=1}^{2}\mu_j^2\varphi_j'(z_j)\right],\\ \sigma_y &= 2\,\mathrm{Re}\left[\sum_{j=1}^{2}\varphi_j'(z_j)\right],\\ \tau_{xy} &= -2\,\mathrm{Re}\left[\sum_{j=1}^{2}\mu_j\varphi_j'(z_j)\right]\end{aligned} \tag{1}$$

where μ_j are the constants of anisotropy obtained by applying generalized Hooke's law, Airy's stress functions and compatibility conditions to anisotropic plate, $\varphi_j'(z_j)$ are the first derivative of Muskhelishvili's complex stress functions $\varphi_j(z_j)$ and $z_j = x + \mu_j y$. To derive the stresses in a finite anisotropic plate, the complex stress functions are derived using Boundary Collocation Method as discussed in following section.

The solution begins with the generation of numbers of collocation points on the boundary of plate and hole as shown in Fig. 1, where $K1 = N1 + 1$, $K2 = K1 + N1$, $K3 = K2 + N1$, $K4 = K3 + N1$ and $N = K4 + N2$, $N1$ and $N2$ are number of points on the side of plate and boundary of the hole respectively. The x and y coordinates of each collocation points are obtained as follows:

$$\begin{aligned}(x_s, y_s) &= (L-l, -h) \quad s = 1\\ &= \left(x_{s-1}, y_{s-1} + \frac{H}{K1-1}\right) \quad 2 \le s \le K1\\ &= \left(x_{s-1} + \frac{L}{K2-1}, y_{s-1}\right) \quad K1+1 \le s \le K2\\ &= \left(x_{s-1}, y_{s-1} - \frac{H}{K3-1}\right) \quad K2+1 \le s \le K3\\ &= \left(x_{s-1} - \frac{L}{K4-1}, y_{s-1}\right) \quad K3+1 \le s \le K4\\ &= \left(\mathrm{Re}(z_s), \mathrm{Im}(z_s)\right) \quad K4+1 \le s \le N\end{aligned} \tag{2}$$

where Re and Im stands for Real and Imaginary part respectively and

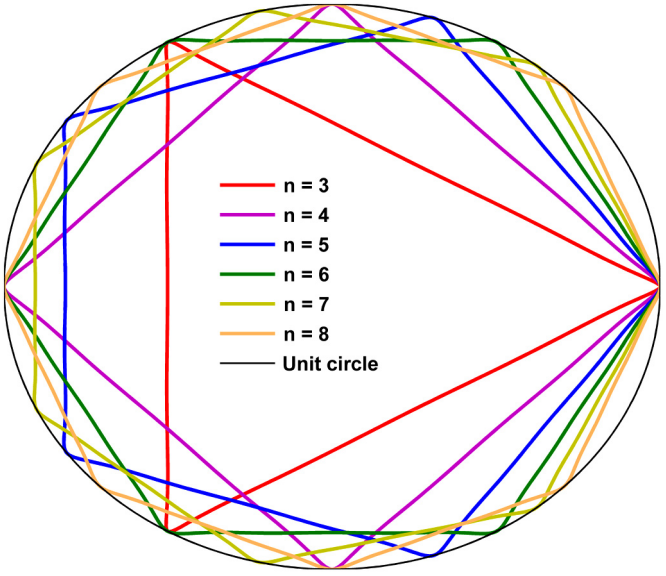

Fig. 2. Geometry of polygonal hole.

$$z_s = R\left[c_0\zeta_s + \sum_k \frac{c_k}{\zeta_s^{p_k}}\right] \tag{3}$$

where R is the size factor, $\zeta_s = e^{i\theta_s}$, $\theta_s = (s - K4 - 1) + 2\pi/N2$, c_0, c_k and p_k are the constants parameters to define different polygonal shape. For the polygonal hole of side n, $c_0 = 1$, $c_k = \frac{(\prod_{j=1}^{k}((j-1)n-2))}{n^k(1-kn)k!}$ and $p_k = kn - 1$. To inscribe the polygonal hole in to a unit circle $R = \frac{1}{1+\sum_k c_k}$ and to orient the polygon at angle α with respect to X axis, the constants c_k are multiplied with $e^{iq_k\alpha}$ where $q_k = p_k + 1$. Eq. (3) is the mapping function that maps the polygonal shape conformally on to a unit circular hole (see Fig. 2).

The geometry of the plate with hole in a complex plane, z-plane is obtained by $z_s = x_s + iy_s$. For the plate made of laminated composite material the plate geometry is defined in z_j-plane, due to affine transformation, as $z_{sj} = x_s + \mu_j y_s$. Considering the constants of anisotropy, the mapping function Eq. (3) takes form

$$z_{sj} = \frac{R}{2}\left[a_j\left(\frac{c_0}{\zeta_s} + \sum_k c_k\zeta_s^{p_k}\right) + b_j\left(c_0\zeta_s + \sum_k \frac{c_k}{\zeta_s^{p_k}}\right)\right] \tag{4}$$

where $a_j = 1 + i\mu_j$ and $b_j = 1 - i\mu_j$.

Multiplying Eq. (4) by ζ^K (K is the maximum power of ζ) and rearranging the terms,

$$\begin{aligned}&Ra_j\sum_k c_k\zeta_{sj}^{p_k+K} + R(a_jc_0)\zeta_{sj}^{K+1} - 2z_{sj}\zeta_{sj}^{K} + R(b_jc_0)\zeta_{sj}^{K-1}\\ &\quad + Rb_j\sum_k c_k\zeta_{sj}^{K-p_k} = 0\end{aligned} \tag{5}$$

Eq. (5) is polynomial equation of ζ that maps all the collocation points of z_j-plane on to ζ_j-plane. Out of $p_k + K$ number of roots of Eq. (5), the one that maps the polygonal shape to unit circular shape is selected and each z_{sj} is mapped to corresponding ζ_{sj} points. On each of this point in ζ_j-plane, the following force boundary conditions are imposed,

$$\begin{aligned}\pm F_x &= \pm S_x(y_s - y_0) = 2\,\mathrm{Re}\sum_{j=1}^{2}\mu_j\left(\varphi_j(\zeta_{js}) - \varphi_j\left(\zeta_j^0\right)\right),\\ \mp F_y &= \mp S_y(x_s - x_0) = 2\,\mathrm{Re}\sum_{j=1}^{2}\left(\varphi_j(\zeta_{js}) - \varphi_j\left(\zeta_j^0\right)\right)\end{aligned} \tag{6}$$

where F_x and F_y are the components of resultant force acting on the segment of the boundary, x_s and y_s are the coordinates of the collocation point, x_0 and y_0 are the coordinates of reference point, $\phi_j(\zeta_j)$ are Muskhelishvili's complex stress functions, ζ_{js} is mapped coordinates for corresponding collocation point z_{js}, S_x and S_y are applied loading on the boundary of the plate and obtained as

$$S_x = \frac{\sigma}{2}\left[(\lambda+1) - \mathrm{Re}\left((\lambda-1)e^{2i\gamma}\right)\right],$$
$$S_y = \frac{\sigma}{2}\left[(\lambda+1) + \mathrm{Re}\left((\lambda-1)e^{2i\gamma}\right)\right] \tag{7}$$

where σ is the applied load per unit length, λ is biaxial loading factor that can be set to 0 or 1 for uniaxial and equi-biaxial loading respectively and γ is load angle.

The complex stress functions $\phi_j(\zeta_j)$ for the finite plate with circular hole can be represented in terms of Laurent series as

$$\varphi_j(\zeta_j) = A_{j0}\ln\zeta_j + \sum_{m=1}^{\infty}\left(A_{jm}\zeta_j^{-m} + B_{jm}\zeta_j^{m}\right) \tag{8}$$

where A_{j0}, A_{jm} and B_{jm} are the unknowns of the series which are to be determined. Here the logarithmic terms are dropped henceforth for the stress free hole conditions and the infinite series is truncated to the finite terms M. Substituting Eq. (8) in to Eq. (6), simplifying and rearranging, the set of boundary equations are obtained and represented in a matrix form as

$$[P]_{(2N\times 4M)}[X]_{(4M\times 1)} = [F]_{(2N\times 1)}, \tag{9}$$

where

$$[P]_{(2N\times 4M)} = \begin{bmatrix} \mu_1(\zeta_1^{-m}-\zeta_{10}^{-m}) & \mu_1(\zeta_1^{m}-\zeta_{10}^{m}) & \mu_2(\zeta_2^{-m}-\zeta_{20}^{-m}) & \mu_2(\zeta_2^{m}-\zeta_{20}^{m}) \\ (\zeta_1^{-m}-\zeta_{10}^{-m}) & (\zeta_1^{m}-\zeta_{10}^{m}) & (\zeta_2^{-m}-\zeta_{20}^{-m}) & (\zeta_2^{m}-\zeta_{20}^{m}) \end{bmatrix},$$
$$[X]_{(4M\times 1)} = \begin{bmatrix} A_{1m} \\ A_{2m} \\ B_{1m} \\ B_{2m} \end{bmatrix}, \tag{10}$$
$$[F]_{(2N\times 1)} = \begin{bmatrix} F_x \\ F_y \end{bmatrix}$$

In Eq. (9), $2N \gg 4M$ and hence a least square method is used to solve the overdetermined system of equations. Once the unknowns of the series stress functions are known, the stress components in the plate can be from Eq. (1).

It is convenient to present the stress components on the perimeter of the polygonal hole in polar coordinates by using following stress transformations:

$$\sigma_\theta + \sigma_r = \sigma_y + \sigma_x,$$
$$\sigma_\theta - \sigma_r + 2i\tau_{r\theta} = (\sigma_y - \sigma_x + 2i\tau_{xy})e^{2i\theta} \tag{11}$$

3. Results and discussion

The mathematical formulation to derive the stresses around the polygonal hole in a finite anisotropic plate is presented in the previous section. A computer programme is prepare to evaluate the stresses in the finite plate based on the formulation. The input to the programme are loading parameters λ and γ, material properties, stacking sequence of laminate, size of finite plate L and H, number of sides of polygon n, orientation of hole α and location of the centre of the hole l and h. The materials considered here are Graphite/Epoxy ($E_1 = 182$ GPa, $E_2 = 10.3$ GPa, $G_{12} = 7.17$ GPa, $\nu_{12} = 0.28$), Glass/Epoxy ($E_1 = 47.4$ GPa, $E_2 = 16.2$ GPa, $G_{12} = 7$ GPa, $\nu_{12} = 0.26$), Plywood ($E_1 = 11.79$ GPa, $E_2 = 5.89$ GPa, $G_{12} = 0.69$ GPa, $\nu_{12} = 0.071$), Boron/Epoxy ($E_1 = 282.77$ GPa, $E_2 = 23.79$ GPa, $G_{12} = 10.35$ GPa, $\nu_{12} = 0.27$) and Isotropic steel ($E = 205$ GPa, $G = 80$ GPa, $\nu = 0.26$).

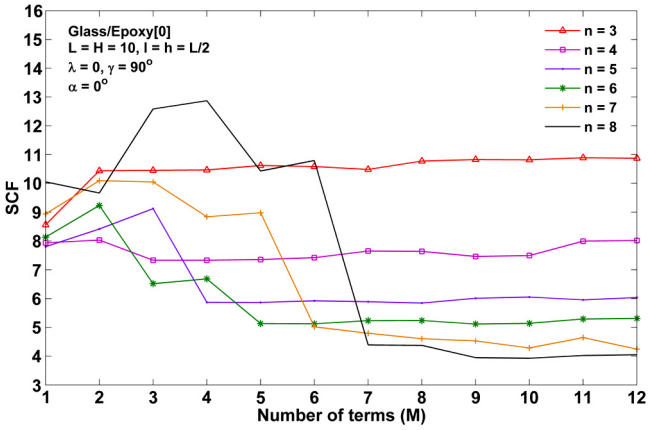

Fig. 3. Convergence of the results.

According to the input, the programme calculates S_x, S_y and constants of anisotropy μ_j. It generates the x and y coordinates of N $(= N_1 + N_2)$ number of collocation points and derives z_j for each point. The mapped coordinate ζ_j are then obtained from z_j and it is further used to generate the system of equations from boundary conditions. An iterative process of increasing the number of terms in series stress functions is employed during the solution of system of equations till the convergence of results. The converged solution is used to derive the stresses around the hole. The stresses around the hole is conveniently derived in polar coordinates using coordinates transformations. Fig. 3 shows the good convergence of the stress concentration factor around different polygonal holes in Glass/Epoxy[0] plate of $L = H = 10$ subjected to uniaxial Y loading.

To validate the present solution, the comparison is made between the results obtained by present method and that of finite element solution through ANSYS as shown in Figs. 4 to 9 for triangular, square, pentagonal, hexagonal, heptagonal and octagonal holes. The exact geometry of the plate with polygonal hole is generated in ANSYS by exporting the coordinates of keypoints through a computer programme. PLANE182 element is used to generate the finite element model in ANSYS as it supports the anisotropic material properties and plane stress condition. The maximum stresses obtained by present method and ANSYS are 10.819 and 11.069 for $n = 3$, 7.49 and 7.74 for $n = 4$, 6.05 and 6.31 for $n = 5$, 5.26 and 5.72 for $n = 6$, 5.11 and 5.25 for $n = 7$ and 4.58 and 4.94 for $n = 8$ respectively. The results are in close agreement with finite element solutions.

The stress distribution around polygonal shaped hole in finite plate subjected to different in-plane loading conditions are shown in Fig. 10(a) for Glass/Epoxy$[0/90]_s$ and Fig. 10(b) for Isotropic plate. It is observed that the stresses in Glass/Epoxy cross ply laminate are more severe than the Isotropic plate for all the loading conditions due to anisotropy of the material.

It is also observed from Fig. 10, that the stress concentration is different at different vertices of the polygonal hole due to its location with respect to the loading direction. For the uniaxial Y loading, the corners at 0° and 180° show the highest stresses compared to other vertices while for uniaxial X loading the corners at 0° and 180° show the least stress concentration compared to other vertices. For the equi-biaxial loading, the stresses are equal at all the corners of all the polygonal hole in isotropic material (Fig. 10(b)) but the same is not true in Glass/Epoxy$[0/90]_s$ plate (Fig. 10(a)) due to material anisotropy except for square hole. The reason of this behavior of square hole may be the location of all the vertices on the axis while the other hole shapes have their ver-

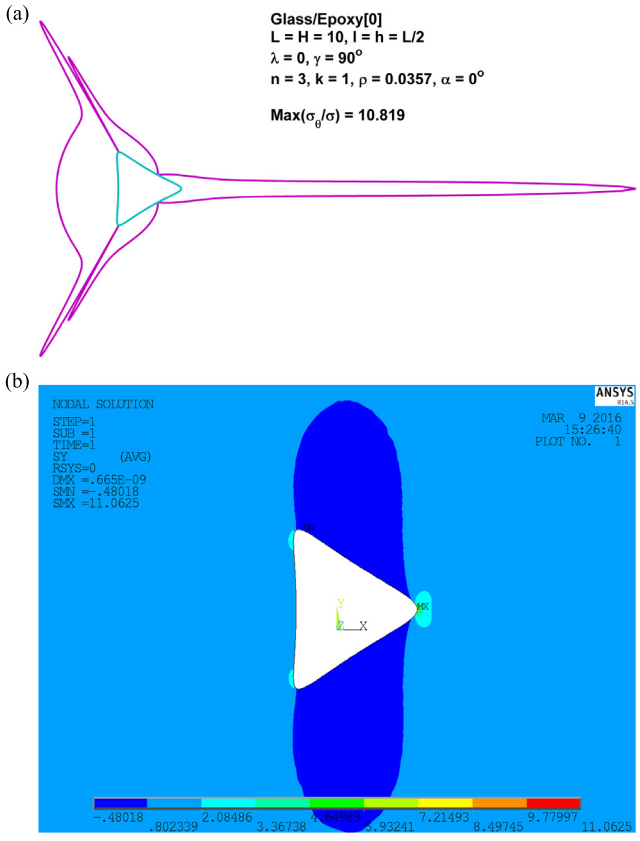

Fig. 4. Comparison of stress distribution around triangular hole in finite anisotropic plate: (a) present method, (b) ANSYS.

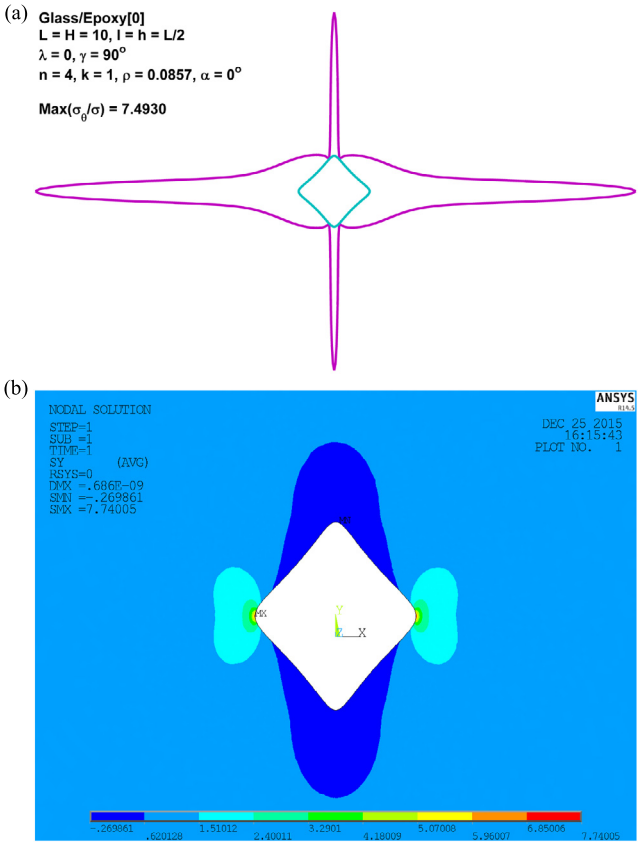

Fig. 5. Comparison of stress distribution around square hole in finite anisotropic plate: (a) present method, (b) ANSYS.

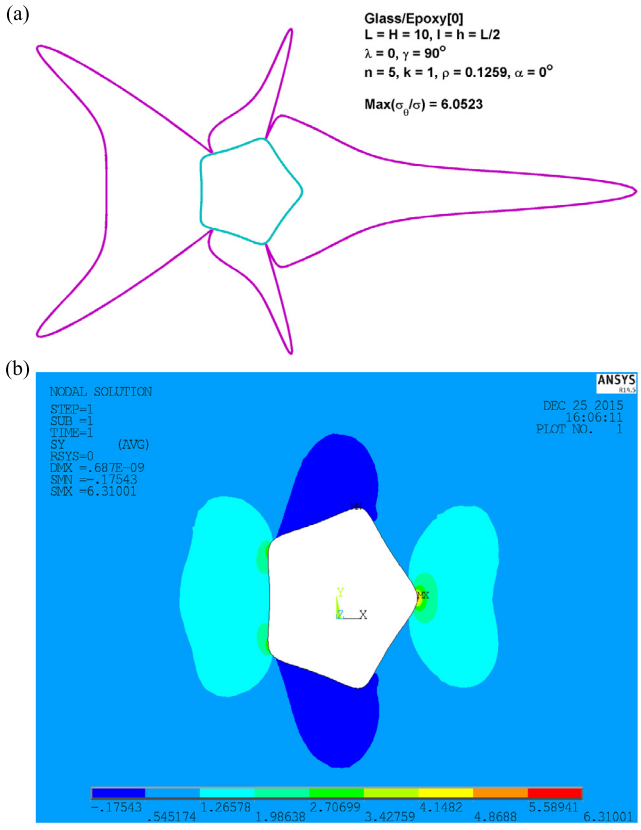

Fig. 6. Comparison of stress distribution around pentagonal hole in finite anisotropic plate: (a) present method, (b) ANSYS.

Fig. 7. Comparison of stress distribution around hexagonal hole in finite anisotropic plate: (a) present method, (b) ANSYS.

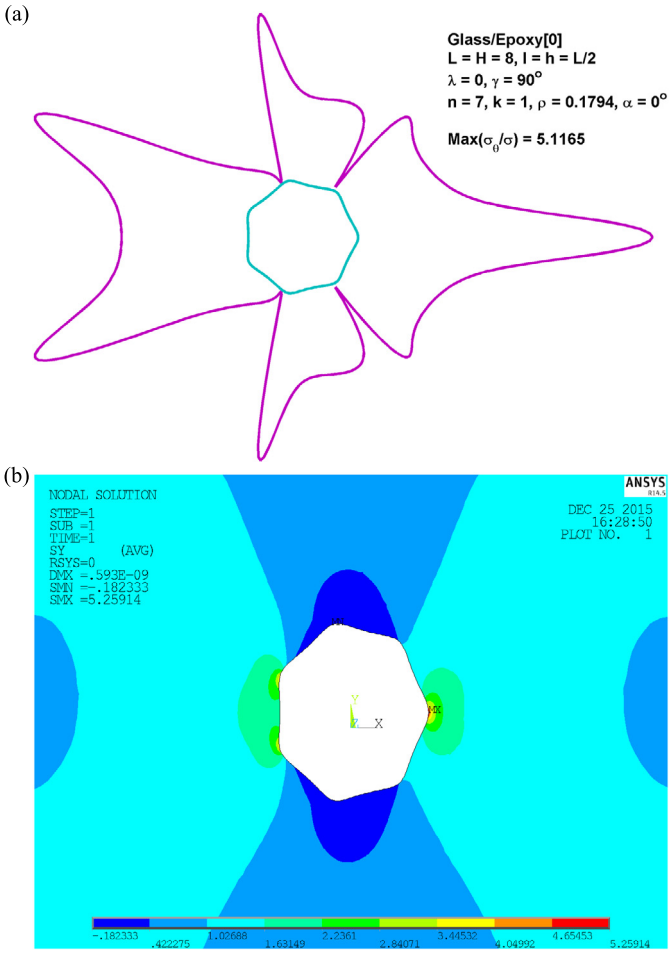

Fig. 8. Comparison of stress distribution around heptagonal hole in finite anisotropic plate: (a) present method, (b) ANSYS.

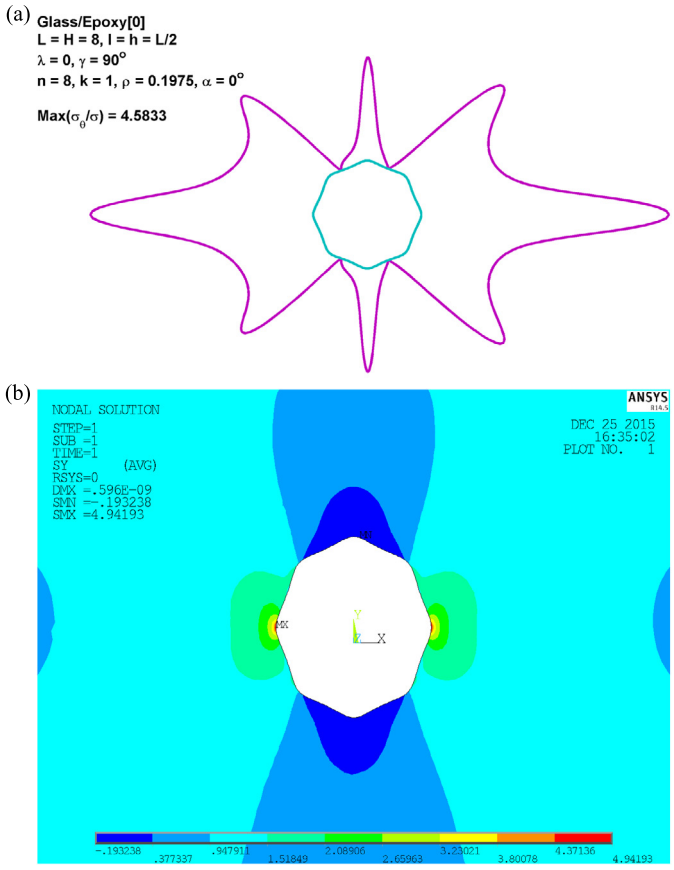

Fig. 9. Comparison of stress distribution around octagonal hole in finite anisotropic plate: (a) present method, (b) ANSYS.

tices at the place other than the axis also. It is seen from Fig. 10, that the vertices are the point of high stress concentration in a plate hence number of vertices, their location and sharpness may affect the stress filed in finite anisotropic plate.

Table 1 shows the values of maximum normalized stresses around the polygonal hole of sides 3, 4, 5, 6 and 7 in the plate of various dimensions and made of Glass/Epoxy[0], Glass/Epoxy[90], Glass/Epoxy$[0/90]_s$ and Isotropic material subjected to uniaxial X, uniaxial Y and equi-biaxial loading. Table 1 shows the effect of plate size, material anisotropy and number of vertices on the stress concentration. It is observed from Table 1 that as the plate size increases the stress concentration decreases and approaches to that of infinite plate. For the comparison purpose, the results of infinite plate are obtained here by using the methodology proposed by Ukadgaonker and Rao [26]. The close agreement of the results obtained by present method for large plate ($L = 100$) with that of infinite plate shows the capability of the present method to produce the satisfactory solutions for infinite plate also.

From Table 1, it is seen that the stress concentration in isotropic plate is higher for Y direction loading and lower for X direction loading for all the shapes of polygons. The same behavior is also observed for Glass/Epoxy cross ply laminate. But due to anisotropy the same is not true for Glass/Epoxy[0] and Glass/Epoxy[90] plate. The stress concentration in Glass/Epoxy[0] is higher for X direction loading while in Glass/Epoxy[90] it is higher for Y direction loading.

It is observed from Table 1 that as the number of vertices increases the stress concentration in a plate decreases gradually for uniaxial Y loading but the same trend is not observed for uniaxial X loading. This can be clearly understood from Fig. 11, which shows the SCF for different polygonal holes in finite plate of Glass/Epoxy cross ply and Isotropic material subjected to uniaxial X and uniaxial Y loading. For uniaxial Y loading, the vertex at 0° i.e. on X axis, shows the highest stresses in all the polygonal hole. While for uniaxial X loading, the vertex of highest stress is not necessarily on X or Y axis but it may be in a plane depending on the geometry of the polygonal shape. As a special case, square hole having all the vertices on the principle axis only, shows the same stress concentration for X and Y direction loading.

The change in number of sides, changes the location of vertices in the plate with respect to loading direction and that alters the stress field. To study the effect of vertices location on stress concentration, the vertices location of a given polygonal hole is altered by three different ways.

In the first case, the vertices location is altered by orienting the hole at angle α varied from 0° to 180° in Glass/Epoxy$[0/90]_s$ finite plate $L = 10$ subjected to uniaxial Y loading. SCF is obtained for different polygonal shapes as shown in Fig. 12. It is observed that the curve is repetitive in nature. The curve repeats at an interval of 90°, 72°, 60° and 45° for square, pentagonal, hexagonal and octagonal shape respectively. This is because of the geometry of the hole shape. It is also noted from Fig. 12 that the SCF is maximum at such orientations when one of the vertices coincide with X axis, as the load is along Y direction.

In the second case, the centrally located hole is kept at 0° orientation and the loading angle γ is varied from 0° to 90°. Here, 0° corresponds to X axial loading while 90° corresponds to Y axial loading. The SCF around different polygonal holes in Glass/Epoxy$[0/90]_s$ and Isotropic material are evaluated for each

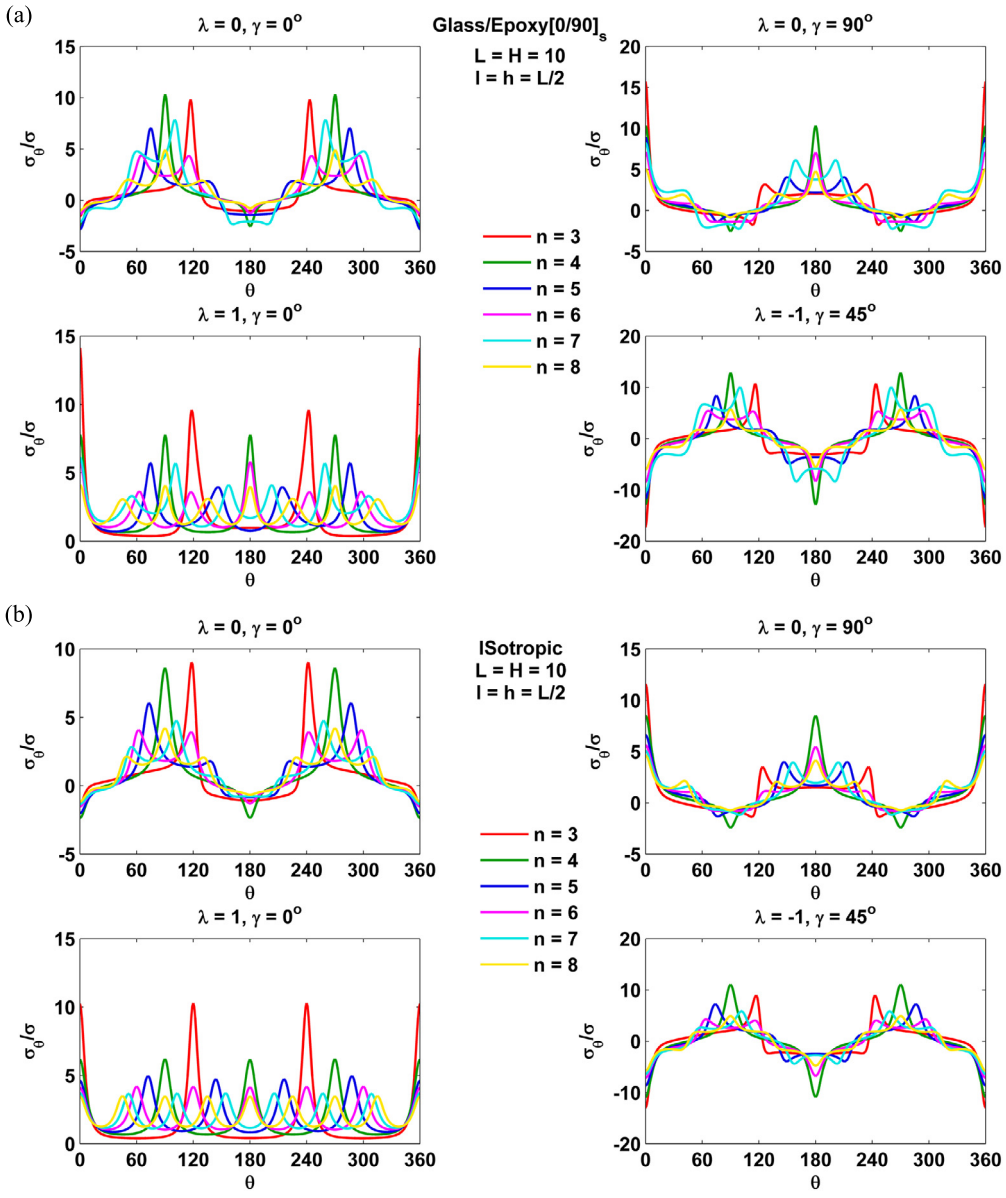

Fig. 10. Stress distribution around polygonal hole in finite plate: (a) Glass/Epoxy plate, (b) Isotropic plate.

Table 1
Stress concentration around centrally located polygonal hole in a plate.

N	*L*	Glass/Epoxy[0]			Glass/Epoxy[90]			Glass/Epoxy[0/90]$_s$			Isotropic		
		Uni-X	Uni-Y	Equi-bi	Uni-X	Uni-Y	Equi-bi	Uni-X	Uni-Y	Equi-bi	Uni-X	Uni-Y	Equi-bi
3	5	14.35	11.87	13.53	9.30	23.24	18.52	11.36	18.61	14.53	10.56	13.44	11.49
	6	13.24	11.37	12.74	8.72	20.92	17.30	10.82	17.60	14.58	9.89	12.66	10.95
	7	12.46	11.14	12.25	8.39	19.51	16.53	10.33	16.15	13.97	9.50	12.19	10.66
	8	12.02	11.02	11.99	8.20	18.59	16.01	10.03	15.29	13.50	9.26	11.90	10.49
	9	11.80	10.95	11.85	8.06	17.98	15.63	9.86	14.74	13.14	9.10	11.70	10.38
	10	11.71	10.95	11.76	7.98	17.51	15.36	9.74	14.41	12.92	8.99	11.56	10.30
	100	10.87	10.11	11.32	7.83	16.46	14.77	9.35	13.52	12.49	8.53	10.97	10.02
	Inf.	10.77	10.09	11.29	7.82	16.55	14.84	9.29	13.55	12.55	8.55	10.92	10.03
4	5	16.41	8.88	10.55	9.05	17.34	9.74	13.04	13.08	8.77	10.90	10.59	7.01
	6	14.97	8.34	9.85	8.34	15.49	9.45	11.88	11.97	8.30	9.90	9.69	6.66
	7	14.03	7.93	9.47	7.95	14.48	9.32	11.27	11.24	8.05	9.33	9.16	6.48
	8	13.52	7.69	9.21	7.81	14.05	9.10	10.79	10.86	7.95	8.97	8.82	6.37
	9	13.13	7.62	9.08	7.64	13.72	9.06	10.55	10.66	7.91	8.73	8.59	6.29
	10	12.95	7.54	8.95	7.54	13.41	9.01	10.39	10.43	7.84	8.55	8.44	6.24
	100	10.75	6.63	8.64	6.63	10.76	8.64	8.83	8.83	7.59	7.44	7.36	6.04
	Inf.	10.33	6.45	8.62	6.45	10.33	8.62	8.53	8.53	7.53	7.08	6.95	6.06

Table 1 (*continued*)

N	L	Glass/Epoxy[0]			Glass/Epoxy[90]			Glass/Epoxy[0/90]$_s$			Isotropic		
		Uni-X	Uni-Y	Equi-bi	Uni-X	Uni-Y	Equi-bi	Uni-X	Uni-Y	Equi-bi	Uni-X	Uni-Y	Equi-bi
5	5	9.77	6.67	7.93	6.89	13.57	6.68	8.28	9.78	6.77	7.83	8.69	5.46
	6	9.11	6.44	7.38	5.97	12.50	6.58	7.69	9.26	6.40	7.00	7.78	5.20
	7	8.69	6.27	7.04	5.74	11.85	6.53	7.39	8.98	6.19	6.53	7.24	5.09
	8	8.48	6.12	6.86	5.60	11.42	6.52	7.15	8.72	6.03	6.28	6.94	5.02
	9	8.34	6.06	6.71	5.50	11.09	6.52	7.02	8.57	5.93	6.13	6.77	4.97
	10	8.21	5.99	6.59	5.43	10.84	6.53	6.89	8.41	5.90	6.04	6.67	4.93
	100	7.15	5.33	5.90	4.82	8.49	6.56	6.03	7.03	5.90	5.27	5.79	4.69
	Inf.	7.03	5.24	5.88	4.76	8.26	6.55	5.96	6.86	5.86	5.20	5.63	4.69
6	5	5.95	6.14	4.87	4.29	11.01	7.32	5.08	8.72	6.51	4.47	6.44	4.57
	6	5.47	5.76	4.70	4.17	10.39	6.89	4.77	8.03	6.25	4.27	6.09	4.41
	7	5.20	5.53	4.61	4.10	9.88	6.58	4.60	7.66	6.11	4.18	5.89	4.31
	8	5.03	5.38	4.55	4.04	9.47	6.33	4.45	7.36	5.98	4.10	5.75	4.25
	9	4.91	5.28	4.51	4.00	9.21	6.25	4.39	7.19	5.89	4.07	5.66	4.20
	10	4.83	5.19	4.48	3.95	9.03	6.16	4.36	7.04	5.83	4.01	5.58	4.17
	100	4.82	4.74	4.25	3.69	7.53	5.45	4.23	6.19	4.93	3.73	5.15	4.00
	Inf.	4.50	4.64	4.17	3.56	7.22	5.51	4.00	6.02	5.02	3.83	4.97	4.01
7	5	6.81	5.15	6.81	4.98	10.19	6.41	5.97	7.68	5.60	5.23	5.88	4.18
	6	6.45	4.77	6.00	4.70	9.18	5.89	5.89	7.05	5.34	5.06	5.54	3.97
	7	6.28	4.55	5.55	4.55	8.58	5.60	5.72	6.54	4.78	4.95	5.36	3.86
	8	6.21	4.43	5.28	4.45	8.19	5.41	5.63	6.33	4.68	4.87	5.23	3.79
	9	6.18	4.34	5.10	4.39	7.92	5.28	5.56	6.19	4.62	4.81	5.15	3.75
	10	6.17	4.29	4.98	4.34	7.72	5.20	5.51	6.08	4.57	4.76	5.08	3.72
	100	6.11	4.20	4.56	4.09	6.64	4.85	5.15	5.54	4.46	4.43	4.65	3.61
	Inf.	6.03	4.27	4.60	4.06	6.60	4.89	5.10	5.52	4.52	4.42	4.57	3.62

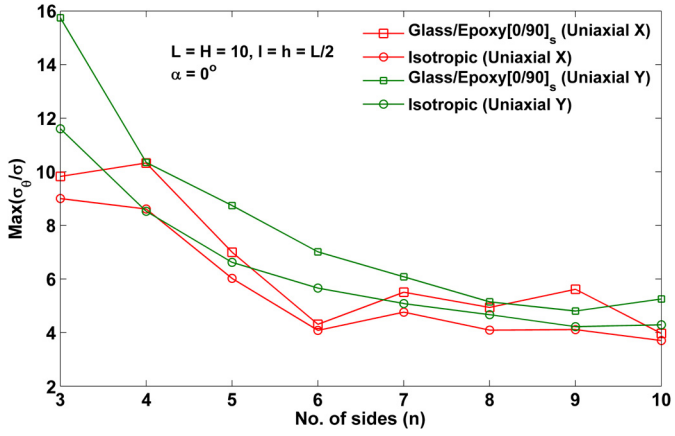

Fig. 11. Effect of number of vertices.

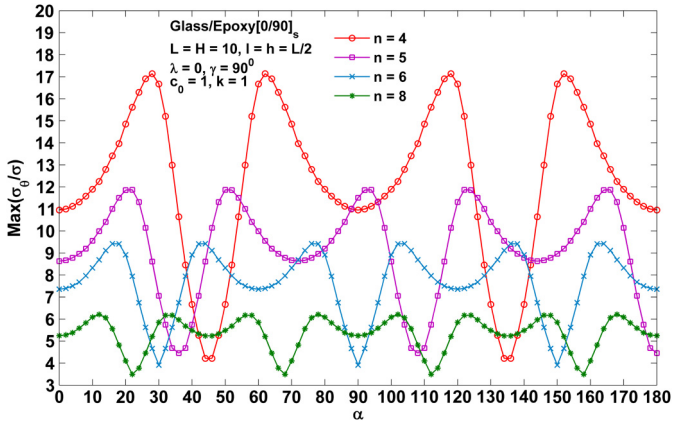

Fig. 12. Effect of hole orientation on stress concentration.

loading angle and plotted as shown in Fig. 13(a) and Fig. 13(b) respectively. The minimum SCF is observed for the load angle ranges from 65° to 70° for different polygonal holes located centrally in a finite plate.

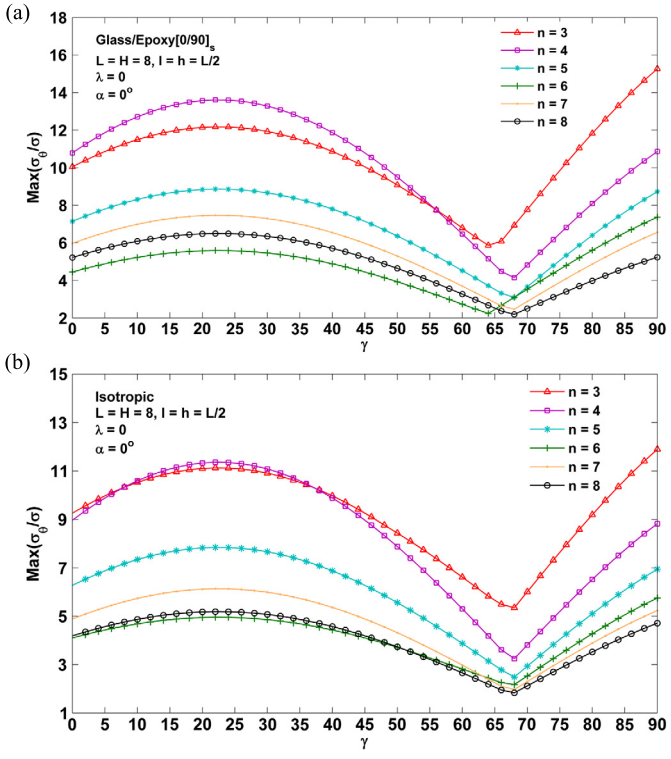

Fig. 13. Effect of load angle on SCF around polygonal hole: (a) Glass/Epoxy, (b) Isotropic.

In the third case, the centre of hole is varied by varying the dimensions l and h with respect to plate boundary in a finite plate. The SCF is evaluated at each position of hole in a plate and a surface plot is produced as shown in Fig. 14 for different polygonal shapes. The X and Y axis show the offset distance of the hole centre from the centre of the plate along length (L) and height (H) respectively. The maximum normalized stress for each location is plotted on Z axis. Fig. 14(a), (b) and (c) show the surface plot for Glass/Epoxy[0] finite plate ($L = H = 10$) subjected to uniaxial Y

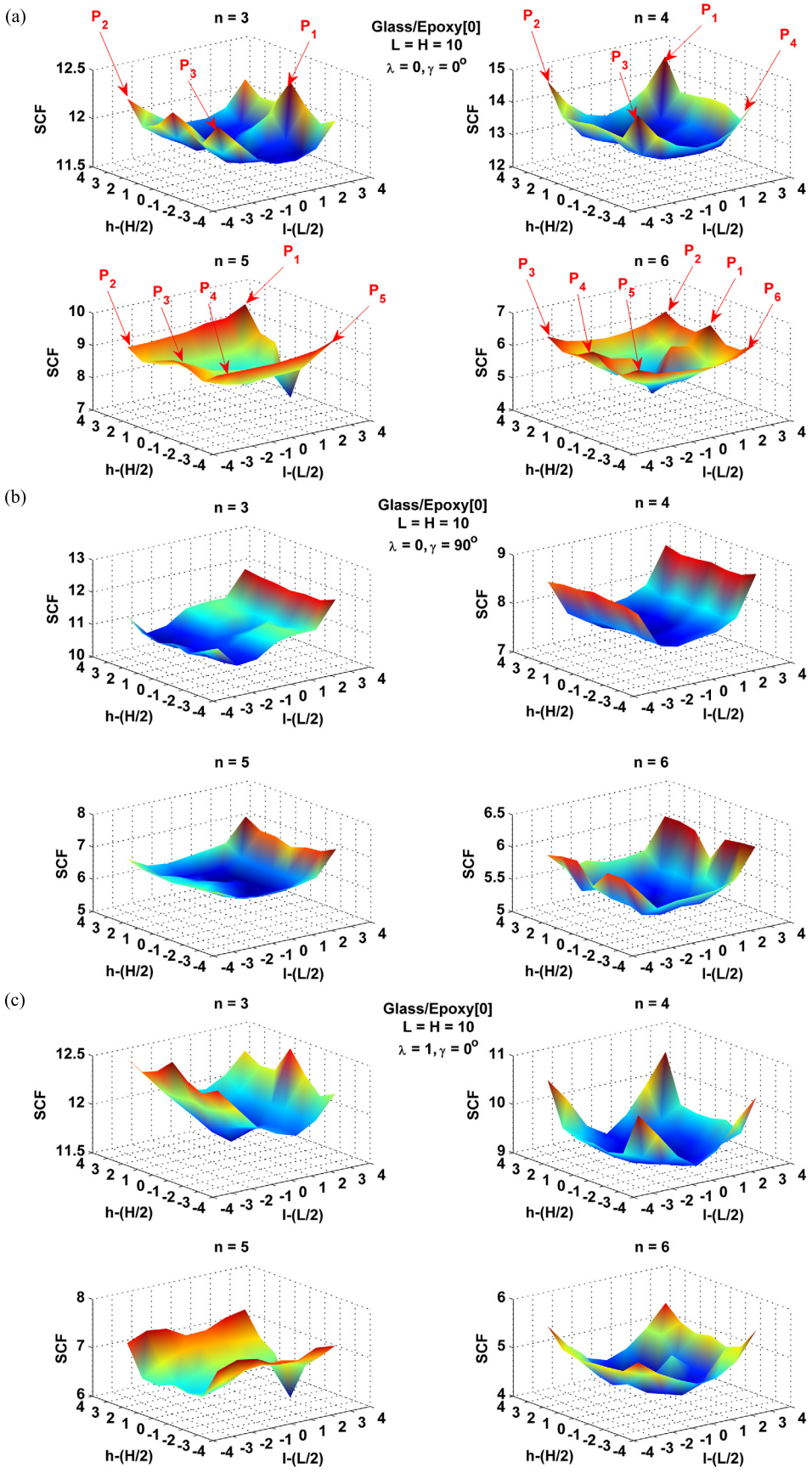

Fig. 14. Effect of hole location on stress concentration around hole: (a) uniaxial X loading, (b) uniaxial Y loading, (c) equi-biaxial loading.

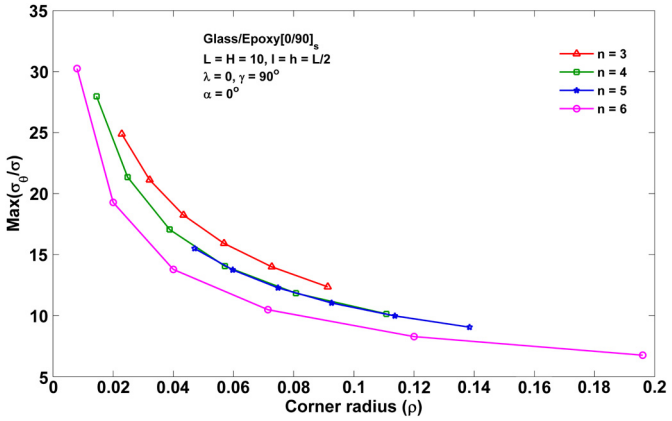

Fig. 15. Effect of corner radius on stress concentration around polygonal hole.

loading, uniaxial X loading and equi-biaxial loading respectively for $n = 3, 4, 5$ and 6. For uniaxial X loading, the pick values of SCF are observed at 3, 4, 5 and 6 locations for $n = 3, 4, 5$ and 6 respectively as shown in Fig. 14(a). But for uniaxial Y loading, the pick values are observed for right most positions of hole in the case of $n = 3$ and $n = 5$ while it is for left most and right most locations of holes with $n = 4$ and $n = 6$ as shown in Fig. 14(b). This may be because triangle and pentagon have only one vertex on X axis (at 0°) and the rest of the vertices are in the plane while square and hexagon have two vertices on X axis (at 0° and 180°) and others are in the plane. From Fig. 14(c), for equi-biaxial loading, it is observed that the high stress concentration locations are similar in square ($n = 4$) and hexagon ($n = 6$), as both the shapes are symmetric with respect to X–Y axis. While for triangle, the high SCF is observed at the locations nearer to left and right edges of the plate and for pentagonal hole, it is at the locations nearer to top and bottom edges of the plate. Form Fig. 14, it can be observed that the corners nearer to the loaded boundary show the high stress concentration.

In addition to the location of corners, the sharpness of the corners may also affect the stress concentration around polygonal hole in anisotropic finite plate. Fig. 15 shows the effect of corner radius on the stress concentration around the polygonal hole of different sides in Glass/Epoxy$[0/90]_s$ plate $L = 10$, subjected to uniaxial Y loading. The corner radius of the polygonal hole is varied by varying the mapping function parameter c_k by considering more number of terms. The corner radius is evaluated based on the formula given by Sharma [7]. It is observed that as the corner radius decrease, the corners become sharper and the stress concentration increases. However for the same corner radius, the SCF for different polygonal hole are different due to the different number of vertices.

Apart from the hole geometry, vertex locations and sharpness of corners, the material anisotropy also affect the stress distribution around the hole. To study this effect, the stress distribution on the perimeter of the different polygonal hole is obtained for Glass/Epoxy laminated plate with different stacking sequences of [0], [90], $[0/90]_s$, $[0_4/\pm 45]_s$, $[90_4/\pm 45]_s$ and $[0_4/\pm 45/90_4]_s$ subjected to uniaxial Y loading as shown in Fig. 16. The stress concentration is minimum in $[0_4/\pm 45]_s$ laminate and maximum in [90] laminate for the uniaxial Y loading. However, for different loading conditions, the behavior may alter.

The effect of ration of E_1/E_2 on SCF around the polygonal hole is shown in Fig. 17. The SCF varies as E_1/E_2 changes for given loading conditions and other material property.

4. Conclusion

The stress distribution around polygonal hole in finite laminated composite plate is obtained using complex variable method in conjunction with boundary collocation method. The attainment of well converged results in time efficient manner and ease of parametric study, make the boundary collocation method suitable for the solution of the present problem. The results obtained by present method are in close agreement with that of finite element solution and the literature. The corners of the polygonal shaped holes are the points of stress concentration in the plate. The number, location and the curvature of the corners significantly affect the stress field in the finite anisotropic plate. The stresses around the polygonal hole is also affected by plate size, material anisotropy and the loading direction. The present generalized solution is capable to produce the satisfactory results for infinite plate by considering large plate size and also for isotropic plate by considering suitable material properties.

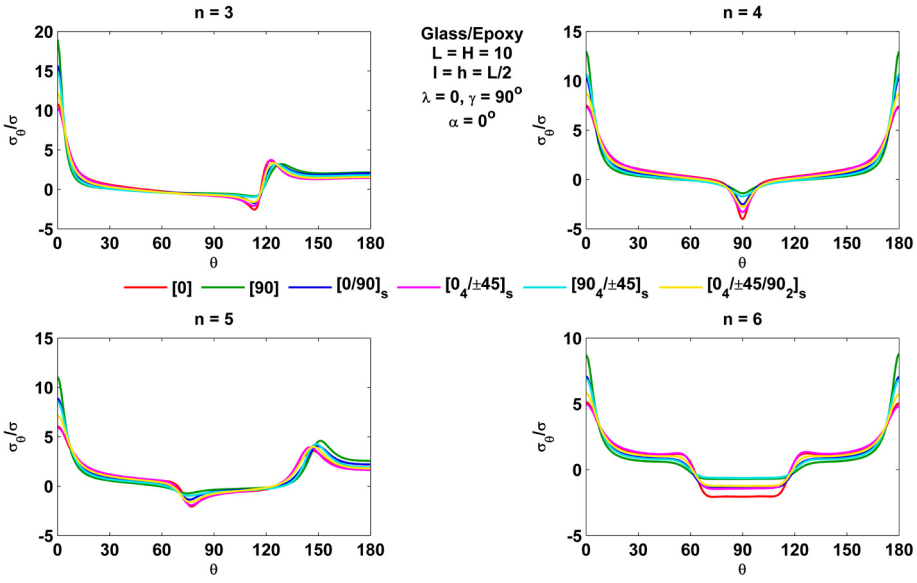

Fig. 16. Effect of stacking sequence on stress distribution around the hole.

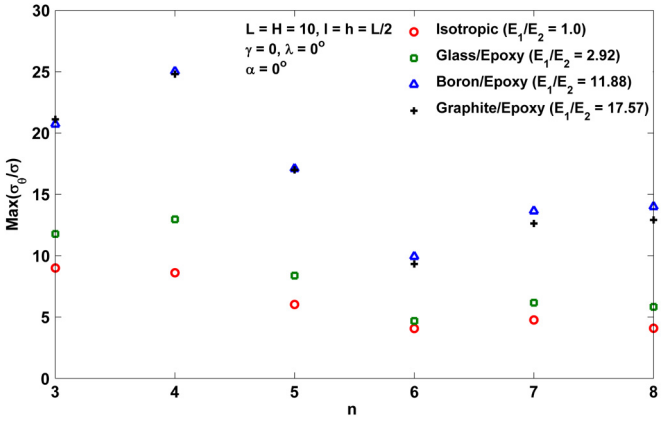

Fig. 17. Effect of anisotropy on stress concentration.

Conflict of interest statement

None declared.

References

[1] H.C. Chen, Special finite element including stress concentration effects of a hole, Finite Elem. Anal. Des. 13 (1993) 249–258.
[2] J. Wang, S.L. Crouch, S.G. Mogilevskaya, A complex boundary integral method for multiple circular holes in an infinite plane, Eng. Anal. Bound. Elem. 27 (2003) 789–802.
[3] N.I. Muskhelishvili, Some Basic Problem of Mathematical Theory of Elasticity, Noordhoof Ltd., The Netherlands, 1963.
[4] G.N. Savin, Stress Distribution Around Holes, Pregamon Press, New York, 1961.
[5] S.G. Lekhnitskii, Anisotropic Plate, Gordon and Breach Science Publishers, New York, 1968.
[6] D.K.N. Rao, M.R. Babu, K.R.N. Reddy, D. Sunil, Stress around square and rectangular cutouts in symmetric laminates, Compos. Struct. 92 (2010) 2845–2859, http://dx.doi.org/10.1016/j.compstruct.2010.04.010.
[7] D.S. Sharma, Stresses around polygonal hole in an infinite laminated composite plate, Eur. J. Mech. A, Solids 54 (2015) 44–52, http://dx.doi.org/10.1016/j.euromechsol.2015.06.004.
[8] D.S. Sharma, Moment distribution around polygonal holes in infinite plate, Int. J. Mech. Sci. 78 (2014) 177–182, http://dx.doi.org/10.1016/j.ijmecsci.2013.10.021.
[9] D.S. Sharma, Stress distribution around polygonal holes, Int. J. Mech. Sci. 65 (2012) 115–124, http://dx.doi.org/10.1016/j.ijmecsci.2013.10.021.
[10] M. Batista, On the stress concentration around a hole in an infinite plate subject to a uniform load at infinity, Int. J. Mech. Sci. 53 (2011) 254–261, http://dx.doi.org/10.1016/j.ijmecsci.2011.01.006.
[11] J. Rezaeepazhand, M. Jafari, Stress concentration in metallic plates with special shaped cutout, Int. J. Mech. Sci. 52 (2010) 96–102, http://dx.doi.org/10.1016/j.ijmecsci.2009.10.013.
[12] J. Rezaeepazhand, M. Jafari, Stress analysis of perforated composite plates with non-circular cutout, Key Eng. Mater. (2008) 4365–4368.
[13] J. Rezaeepazhand, M. Jafari, Stress analysis of perforated composite plates, Compos. Struct. 71 (2005) 463–468, http://dx.doi.org/10.1016/j.compstruct.2005.09.017.
[14] J. Daoust, S.V. Hoa, An analytical solution for anisotropic plates containing triangular holes, Compos. Struct. 19 (1991) 107–130.
[15] J.M. Ogonowski, Analytical study of finite geometry plates with stress concentrations, in: AIAA/ASME/ASCE/AHS 21st SDN Conf., Washington, 1980.
[16] E. Madenci, L. Ileri, J.N. Kudva, Analysis of finite composite laminates with holes, Int. J. Solids Struct. 30 (1993) 825–834.
[17] X. Xiwu, S. Liangxin, F. Xuqi, Stress concentration of finite composite laminates with elliptical hole, Comput. Struct. 57 (1995) 29–34.
[18] C.C. Lin, C.C. Ko, Stress and strength analysis of finite composite laminate with elliptical hole, J. Compos. Mater. 22 (1988) 373–385.
[19] A.J. Durelli, V.J. Parks, V.J. Lopardo, Stresses and finite strains around an elliptical hole in finite plates subjected to uniform load, Int. J. Non-Linear Mech. 5 (1970) 397–411.
[20] Z. Pan, Y. Cheng, J. Liu, Stress analysis of a finite plate with a rectangular hole subjected to uniaxial tension using modified stress functions, Int. J. Mech. Sci. 75 (2013) 265–277, http://dx.doi.org/10.1016/j.ijmecsci.2013.06.014.
[21] M. Jafari, E. Ardalani, Stress concentration in finite metallic plates with regular holes, Int. J. Mech. Sci. 106 (2016) 220–230.
[22] M.M. Chauhan, D.S. Sharma, Stresses in finite anisotropic plate weakened by rectangular hole, Int. J. Mech. Sci. 101–102 (2015) 272–279, http://dx.doi.org/10.1016/j.ijmecsci.2015.08.007.
[23] M.M. Chauhan, D.S. Sharma, J.M. Dave, Stress intensity factor for hypocycloidal hole in finite plate, Theor. Appl. Fract. Mech. 82 (2016) 59–68.
[24] O.L. Bowie, D. Neal, A modified mapping collocation technique for accurate calculation of stress intensity factors, Int. J. Fract. Mech. 6 (1970) 199–206.
[25] J.C. Newman, An improved method of collocation for the stress analysis of cracked plates with various shaped boundaries, NASA Tech. Note. D6376, 1971.
[26] V.G. Ukadgaonker, D.K.N. Rao, A general solution for stresses around holes in symmetric laminates under inplane loading, Compos. Struct. 49 (2000) 339–354.